

which the KDP loss is not significant, there may be some advantage in operating at reduced temperature. However, thermal strain and the higher dielectric constant may prove troublesome<sup>24</sup> at low temperature.

There are at least two KDP isomorphs— $\text{KD}_2\text{PO}_4$  and  $\text{KH}_2\text{AsO}_4$ —that require less dc voltage than KDP to produce a given phase retardation at room tempera-

ture.<sup>25</sup> If the microwave loss in these materials is sufficiently low, and if the microwave dielectric constant does not indicate any dispersion, these substances may provide a means for avoiding some of the problems involved in operating at reduced temperature.

<sup>25</sup> *American Institute of Physics Handbook*, edited by Dwight E. Gray (McGraw-Hill Book Company, New York, 1957).

## Far Infrared Antiferromagnetic Resonance in MnO and NiO†

A. J. SIEVERS, III,\* AND M. TINKHAM

*Department of Physics, University of California, Berkeley, California*

(Received 27 September 1962)

The uniaxial dipolar anisotropy in antiferromagnetic MnO and NiO aligns the two opposing sublattice moments in an easy (111) plane. The two normal modes for small oscillations of the sublattice magnetizations about a preferred direction within this plane are both nondegenerate and linearly polarized. The high-frequency mode has been observed at low temperatures (2°K) at 27.5 and 36.6  $\text{cm}^{-1}$  in MnO and NiO, respectively. In agreement with the unobservably small second-order Zeeman shift expected for these nondegenerate modes, a 10.7-kOe field was found to have no effect on the observed resonance frequencies. Increasing the sample temperature decreases the frequency of the mode in each case. The experimental temperature dependence of the antiferromagnetic resonance frequency can be accounted for by present theories only if an anomalous temperature dependence, previously found from neutron-diffraction data, is assumed for the temperature dependence of the sublattice magnetization.

### I. INTRODUCTION

BECAUSE coherent sources at present do not extend through the far infrared region of the electromagnetic spectrum, two very different experimental methods are used to examine the high-frequency properties of magnetic compounds. They consist of tuning the magnetic absorption to another frequency region with large magnetic fields<sup>1</sup> or using incoherent sources.<sup>2</sup> We have used the second method, namely, incoherent sources and optical techniques, to obtain transmission measurements on the antiferromagnetic resonances in manganese oxide<sup>3</sup> (MnO) and nickel oxide (NiO) under different experimental conditions.

In antiferromagnetic MnO and NiO, the most important source of anisotropy energy is the long-range magnetic-dipole interaction. Because  $L=0$  in  $\text{Mn}^{2+}$  and because the lowest level of  $\text{Ni}^{2+}$  in NiO is an orbital singlet, the interaction of individual magnetic ions with the crystalline electric field from the slightly distorted octahedron of oxygen ions is of far lesser importance than the dipolar anisotropy.

The anisotropy energy from dipolar interactions has been calculated by Kaplan<sup>4</sup> for magnetic ions in a two-

sublattice NaCl structure. Keffer and O'Sullivan<sup>5</sup> have computed the dipolar anisotropy for the general case of ordering of the second kind, but they suggest that, due to lattice distortion, the general eight-sublattice model can be replaced by a two-sublattice one, in which the spins are constrained by dipolar and exchange forces to point parallel to the (111) planes and constrained by weaker anisotropy to a threefold set of axes within these planes. It is the Keffer and O'Sullivan two-sublattice model using the Kaplan dipolar computation that we have compared with our experimental results.

### II. INFRARED PROPERTIES OF MnO AND NiO

The magnetic dipole-dipole interaction in NaCl-structure antiferromagnets, such as MnO and NiO, produces an unusual uniaxial anisotropy energy in which the uniaxis is the hard axis.<sup>4</sup> This easy plane anisotropy causes the uniform precession modes to be very different from those for oscillations about an easy uniaxis. The two modes in MnO and NiO are found to be nondegenerate and linearly polarized, whereas the two normal modes are degenerate and circularly polarized for the case of an easy-uniaxis antiferromagnet. Let us consider these nondegenerate modes in more detail. Since the dipolar anisotropy only determines a plane, the actual easy direction within the plane is determined by higher-order anisotropy terms. Thus for small oscillations at  $k=0$ , the sublattices appear to move in the exchange field, plus an anisotropy

\* Present address: Laboratory for Atomic and Solid State Physics, Cornell University, Ithaca, New York.

† Supported in part by the U. S. Office of Naval Research, The National Science Foundation, and the Alfred P. Sloan Foundation.

<sup>1</sup> S. Foner, *J. Phys. Radium* **20**, 336 (1959).

<sup>2</sup> R. C. Ohlmann and M. Tinkham, *Phys. Rev.* **123**, 425 (1961).

<sup>3</sup> A preliminary report of these results has been given: F. Keffer, A. J. Sievers, III, and M. Tinkham, *J. Appl. Phys.* **32**, 65S (1961).

<sup>4</sup> J. Kaplan, *J. Chem. Phys.* **22**, 1709 (1954).

<sup>5</sup> F. Keffer and W. O'Sullivan, *Phys. Rev.* **108**, 637 (1957).

field of orthorhombic symmetry. The normal mode frequencies for such an anisotropy field have been found by Keffer and Kittel.<sup>6</sup>

Taking  $\omega_{a_1}$ ,  $\omega_{a_2}$  for the frequencies corresponding to the dipolar anisotropy and the higher-order anisotropy, respectively, the two resonance frequencies are

$$\begin{aligned}\omega_1 &= (2\omega_e\omega_{a_1})^{1/2} = (12\lambda K)^{1/2}, \\ \omega_2 &= (2\omega_e\omega_{a_2})^{1/2},\end{aligned}\quad (1)$$

for  $\omega_e \gg \omega_{a_1}$ ,  $\omega_{a_2}$ . In (1),  $\omega_e = \gamma\lambda M$  and  $\omega_{a_1} = 6\gamma K/M$ , where  $\gamma$  is the sublattice gyromagnetic ratio,  $\lambda$  is the molecular-field constant,  $M$  is the sublattice magnetization, and  $K$  is the dipolar anisotropy constant, as given by Kaplan. The dipolar anisotropy is thought to be much larger than the in-plane anisotropy and only the high-frequency mode is expected in the far infrared.<sup>5</sup> The corresponding rf susceptibilities are

$$\begin{aligned}\chi_y'(\omega) &= -2\gamma M\omega_{a_1}/(\omega^2 - \omega_1^2), \\ \chi_x'(\omega) &= -2\gamma M\omega_{a_2}/(\omega^2 - \omega_2^2).\end{aligned}\quad (2)$$

Notice that the frequency and susceptibility of each mode is determined by a different anisotropy field. From the equations of motion, a pictorial description of the two modes can be obtained. Such a diagram of the high-frequency mode  $\omega_1$  is shown in Fig. 1. In (a) the constant-length sublattice vectors precess in opposite directions and trace out elliptical paths on the surface of a sphere. Looking along the  $z$  axis in (b), the motion of the sublattices produces an oscillating linear magnetic moment in the ( $y$ ) easy direction. The low-frequency mode is similar in appearance but the axis of the ellipse is rotated  $90^\circ$ , and the oscillating linear magnetic moment is in the ( $x$ ) hard direction. Both sublattices in each mode give rise to oscillating magnetic  $z$  components; however, at  $k=0$  there is no *net* oscillating  $z$  component to interact with a  $z$ -directed rf field.

Since only the high-frequency mode has been studied, let us consider its properties further. For narrow lines the integrated absorption can be easily obtained from (2) by using one of the Kramers-Kronig relations.<sup>7</sup> The integrated absorption is found to be

$$\chi_y''(\omega_1)\Delta\omega = \pi\gamma M_0\omega_{a_1}/\omega_1 \quad (3)$$

for the high-frequency mode. The contribution of this mode to the perpendicular static susceptibility is

$$\chi_y(0) = (2/\pi)[\chi_y''(\omega_1)(\Delta\omega/\omega_1)] = 1/\lambda. \quad (4)$$

A well-known result for static fields acting on antiferromagnetics is that  $\chi_{\perp} = 1/\lambda$ . We see that the mode above accounts for the entire static susceptibility in the  $y$  direction.

For a static magnetic field applied to the crystal along

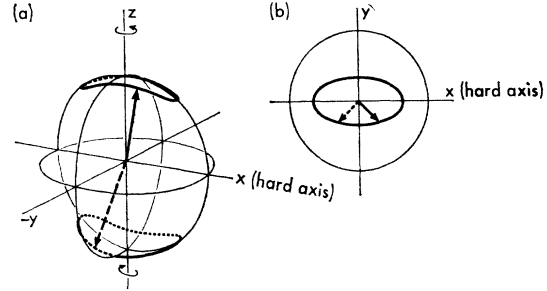


FIG. 1. Infrared normal mode. The up and down sublattices precess in opposite directions giving rise to an oscillating  $y$  component. The low-frequency mode (not shown) has the same form but gives rise to an oscillating  $x$  component of magnetization.

the  $z$  axis, the high-frequency mode shifts. For  $\omega_H = \gamma H_z \ll \omega_2$  an approximate expression is<sup>6,8</sup>

$$\Delta\omega/\omega \approx \frac{3}{2}(\omega_H/\omega_1)^2. \quad (5)$$

Hence, application of an external field along the  $z$  axis produces a second-order Zeeman shift. The reason that application of a magnetic field much smaller than the resonance field increases the resonance frequency only by quadratic and higher terms is that the mode is non-degenerate. According to Fig. 1, the high-frequency mode has an oscillating moment in the ( $111$ ) plane. It is the coupling of this moment to the oscillating component of the infrared radiation that produces the resonance absorption. Because there is no time average moment in this mode, the applied field  $H$  must first create a moment before it can shift the frequency; hence, a quadratic shift in  $H$  results.

Another interesting feature of the easy plane anisotropy antiferromagnets is that only one "flop field" should be present. The flop field is that value of  $H$  which, when applied parallel to the preferred spin direction, causes the spins suddenly to rotate to a position orthogonal to  $H$ . As long as the component of the applied field in the ( $111$ ) plane can overcome the in-plane anisotropy, the spins will always be perpendicular to the applied field, irrespective of its direction, because they are now free to orient within this plane. Thus, no discontinuous behavior is expected at the much higher critical field  $H_c = \omega_1/\gamma$ .

### III. EXPERIMENTAL RESULTS

Because very little energy is available in the far infrared region from conventional broad-band sources, experimental technique plays an important role in any investigation. The far infrared monochromator used in our experiments has been described in detail by Ohlmann.<sup>2</sup> The cryostat for low-temperature was of simple design and has been described elsewhere.<sup>9</sup>

<sup>8</sup> A. J. Sievers, III, thesis, University of California, 1962 (unpublished).

<sup>9</sup> A. J. Sievers, III, and M. Tinkham, Phys. Rev. **124**, 321 (1961).

<sup>6</sup> F. Keffer and C. Kittel, Phys. Rev. **85**, 329 (1952).

<sup>7</sup> M. Tinkham, Phys. Rev. **124**, 311 (1961).

### Manganese Oxide

Transmission measurements were made on a 0.23-mm thick pressed-powder MnO disk at 2°K. Measurements were also made on an equal amount of MnO powder in a paraffin matrix. In each case the transmission at 2°K was monotonically decreasing from 10 cm<sup>-1</sup> to 100 cm<sup>-1</sup> except for a sharp absorption at

$$\omega_1 = 27.5 \pm 0.3 \text{ cm}^{-1} \quad (\text{experimental}).$$

From Eq. (1), the predicted frequency is

$$\omega_1 = 29.0 \text{ cm}^{-1} \quad (\text{calculated}).$$

In predicting this frequency,  $\chi_1$  was taken<sup>3</sup> as  $4.74 \times 10^{-4}$  emu/cm<sup>3</sup> and  $K$ , allowing for zero point motion of the sublattice magnetization, was taken as  $3.82 \times 10^6$  ergs/cm<sup>3</sup>.<sup>3,8</sup>

The observed width of the resonance line at one-half maximum absorption was 0.9 cm<sup>-1</sup>, and the corresponding width of the monochromator resolution function was 0.75 cm<sup>-1</sup>. Assuming Gaussian profiles for both the absorption line and the resolution function, the true half-width appears to be

$$\Delta\omega \leq 0.5 \text{ cm}^{-1}.$$

As we have a relation, Eq. (4), connecting the absorption strength of the line to the perpendicular static susceptibility, a check on the  $\chi''(\omega)$  calculated from transmission measurements is possible. Our estimated powder absorption strength of the high-frequency antiferromagnetic resonance is

$$S_p = \chi_p''(\omega_1)\Delta\omega = 0.47 \times 10^{-3} \text{ emu cm}^{-3} \text{ cm}^{-1}.$$

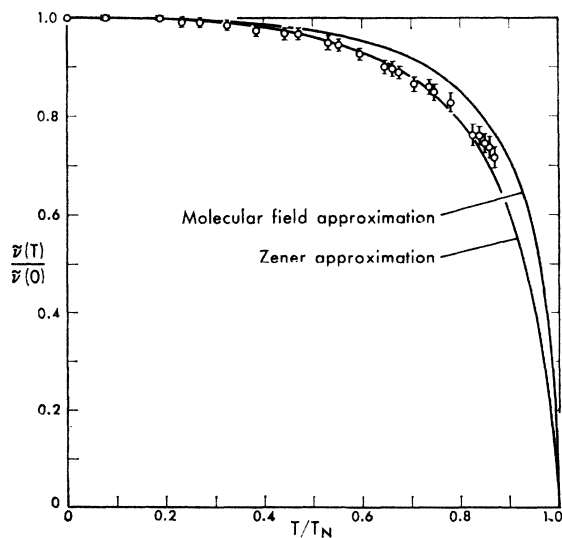


FIG. 2. Temperature dependence of antiferromagnetic resonance in MnO compared with the dependence predicted by the molecular field and also the Zener approximation. The square root of the neutron-scattering intensity has been used for the temperature dependence of the sublattice magnetization, as discussed in Sec. IV.

With this strength and Eq. (4), the contribution of this mode to the static susceptibility is estimated to be

$$\chi_{py}'(0) = 1.1 \times 10^{-4} \text{ emu cm}^{-3}. \quad (6)$$

Our results can be compared with available dc measurements by noting that

$$\chi_{py}' = \frac{1}{2}\chi_{p1} = \frac{1}{3}\chi_1,$$

where  $p$  refers to powder average. From reference 3,

$$\chi_{py}' = 1.58 \times 10^{-4} \text{ emu cm}^{-3}. \quad (7)$$

Considering that the absorption line was not completely resolved, the agreement between our value [see Eq. (6)] and dc measurement [see Eq. (7)] is reasonably good.

The application of a 10 700-Oe magnetic field to the powder MnO sample produced no observable shift or change in the resonance frequency.

When a magnetic field is applied to a powder sample, the line is broadened because of the random directions that the various domains make with respect to this field. A measure of this broadening is the shift in resonance frequency for those domains with  $H$  along the symmetry axis. From our examination of the field dependence of the resonance frequency, given by Eq. (5), the relative shift for MnO is expected to be

$$\Delta\omega/\omega_1 \approx 0.002.$$

We cannot measure this small change because it corresponds to only 5% of the instrumental linewidth.

Higher temperature measurements up to 130°K ( $T_N = 120^\circ\text{K}$ ) were made by placing the sample in a metal transmission Dewar separate from the detector cryostat. Temperatures above 77°K were maintained by attaching an adjustable heater to the sample holder, which was also connected to the nitrogen bath by a copper braid. At the highest temperatures and lowest frequencies, temperature fluctuations lead to errors of up to 0.3 cm<sup>-1</sup> in the resonant frequency. To obtain intermediate temperatures up to 77°K, gas from a liquid-helium cryostat was used to cool the sample holder to 5 or 10°K. When the refrigerant was turned off, the inner assembly would slowly approach the equilibrium temperature of the liquid nitrogen in the surrounding tank and heat shield. A temperature change of 2° was measured in the time required to sweep through the line at 17°K, while at 63°K the measured difference was 0.2°K. Because of the small slope of frequency-vs-temperature curve in this range, a temperature controller was not required. The experimental temperature dependence of the antiferromagnetic resonance frequency is given in Fig. 2. Some experimental points are a mean from two or more runs, as six different sweeps through temperature were made using this technique.

### Nickel Oxide

The first observation of far infrared antiferromagnetic resonance in nickel oxide was made by Kondoh<sup>10</sup> at temperatures from 90 to 470°K. We have extended the measurements to lower temperatures and also examined the effect of a 10 700-Oe magnetic field applied to a single-crystal sample. Transmission measurements at 2°K on a single crystal, cut perpendicular to the [111] direction, revealed an absorption maximum at

$$\omega_1 = 36.6 \pm 0.3 \text{ cm}^{-1} \quad (\text{experimental}).$$

As in the case of MnO, we compare our experimental value to that given by Eq. (1). In this case, we take<sup>11</sup>  $\chi_1 = 0.715 \times 10^{-4} \text{ emu/cm}^3$  and  $K = 1.02 \times 10^6 \text{ ergs/cm}^3$ . The theoretical resonance frequency is then

$$\omega_1 = 43.0 \text{ cm}^{-1} \quad (\text{calculated}).$$

The experimental linewidth was  $0.9 \text{ cm}^{-1}$ , and the width of the resolution function was  $0.7 \text{ cm}^{-1}$ . We estimate the upper bound on the true linewidth to be

$$\Delta\omega \leq 0.6 \text{ cm}^{-1}.$$

Calculating  $\chi''(\omega_1)$  from the transmission measurements and, from this, estimating a line strength

$$S_y = 0.81 \times 10^{-3} \text{ emu cm}^{-3} \text{ cm}^{-1},$$

the contribution to the dc susceptibility from this resonance mode is found to be

$$\chi_y'(0) = 0.17 \times 10^{-4} \text{ emu cm}^{-3}. \quad (8)$$

The accepted dc perpendicular susceptibility is<sup>11</sup>

$$\chi_1 = 0.715 \times 10^{-4} \text{ emu cm}^{-3}. \quad (9)$$

There is some ambiguity in comparing our susceptibility value Eq. (8), with the value Eq. (9), because no attempt has been made to orient the domains in our single-crystal sample. On the other hand, Roth and Slack<sup>11</sup> obtained their susceptibility value from a stress-annealed crystal which they estimate had 98.7% of the domains oriented. The large number (12) of different domain orientations possible in a single crystal suggests that a spherical average of the true perpendicular susceptibility should be compared with our multidomain susceptibility result. A spherical average of Eq. (9) gives

$$\chi_{Dy} \approx \frac{1}{3}\chi_1 = 0.238 \times 10^{-4} \text{ emu cm}^{-3}. \quad (10)$$

The agreement of expressions (8) and (10) is satisfactory.

More accurate temperature-dependence measurements of the resonance frequency are possible in nickel oxide than in MnO because the Néel temperature (523°K) is above room temperature. Temperature control of the sample was maintained by placing the

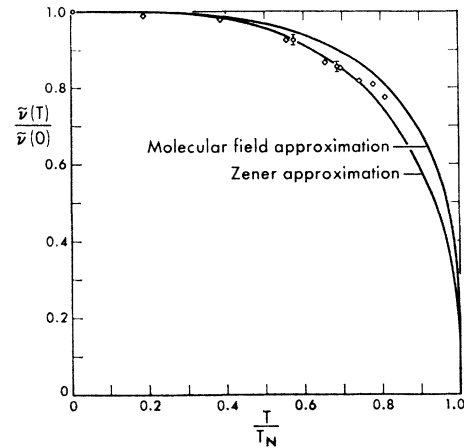


FIG. 3. Temperature dependence of antiferromagnetic resonance in NiO compared with the dependence predicted by the molecular-field and the Zener approximation. The square root of neutron-scattering intensity data has been used for the temperature dependence of the sublattice magnetization, as discussed in Sec. IV. The diamond-shaped points were obtained by Kondoh (reference 10).

sample, heater, and thermocouple in an aluminum cylinder which was inserted into a  $\frac{1}{2}$ -in. light-pipe gap between monochromator and detector. The experimental points are in good agreement with the results of Kondoh.<sup>10</sup> The results of both far infrared measurements are shown in Fig. 3.

We have also made a high-resolution measurement of the absorption at 300°K. An absorption maximum was observed at a resonance frequency of  $34.1 \pm 0.3 \text{ cm}^{-1}$  with a linewidth of  $2.4 \text{ cm}^{-1}$ . The width of the resolution function of the monochromator was only  $0.9 \text{ cm}^{-1}$ . The true width is then approximately

$$\Delta\omega \approx 2.3 \text{ cm}^{-1}.$$

The absorption strength at 300°K was found to be

$$S_y = 0.90 \times 10^{-3} \text{ emu cm}^{-3} \text{ cm}^{-1}$$

giving a contribution to the static susceptibility of

$$\chi_y'(0) = 0.18 \times 10^{-4} \text{ emu cm}^{-3}.$$

It is encouraging to find almost exact agreement between this result and the low-temperature value,  $\chi_y = 0.17 \times 10^{-4} \text{ emu cm}^{-3}$ .

### IV. DISCUSSION

Because the molecular field constant  $\lambda$  is expected to be nearly independent of temperature, Eq. (1) shows that the temperature dependence of the resonance frequency is proportional to the square root of the temperature dependence of the anisotropy constant. The anisotropy constants, however, are expected to vary with a power of the sublattice magnetization. We have attempted to fit our resonance data to a power of a modified Brillouin function of the appropriate spin,

<sup>10</sup> H. Kondoh, J. Phys. Soc. (Japan) **15**, 1970 (1960).

<sup>11</sup> W. L. Roth and G. A. Slack, J. Appl. Phys. **31**, 352S (1960).

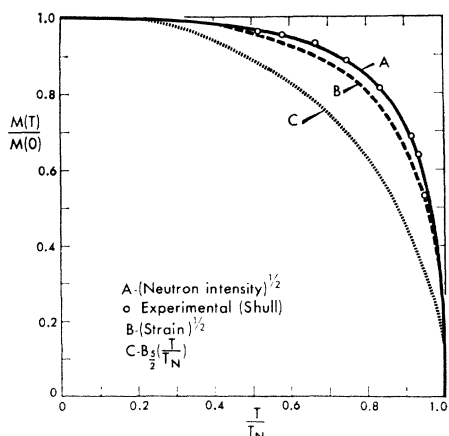


FIG. 4. Temperature dependence of the sublattice magnetization in MnO as given by the square root of the neutron intensity and the square root of the magnetoelastic strain.  $B_{5/2}(T/T_N)$  is shown for comparison.

$B_S(T/T_N)$ . The square root of  $B_{5/2}(T/T_N)$  appears to fit the MnO data quite well.<sup>12</sup> This exponent  $n = \frac{1}{2}$ , is to be contrasted with the exponents given by the Zener<sup>13,14</sup> and molecular field approximations,<sup>15</sup> namely,  $n = \frac{3}{2}$  and 1, respectively. Two explanations for the difference in power law have been considered. Either the temperature dependence of the anisotropy constant follows an unexpected power law or else the sublattice magnetization does not follow  $B_S(T/T_N)$ . The NiO data, when compared with MnO, lead us to prefer the latter explanation. For, if the temperature dependence of the resonance frequency for NiO follows a power law of  $B_1(T/T_N)$ , the experimental points of Fig. 3 indicate that the exponent is between  $n = \frac{1}{2}$  and  $n = 1$ , rather than  $\frac{1}{2}$ . Because the source of anisotropy is the same for each material, the anisotropy power law is also expected to be the same. The results then suggest that the sublattice magnetizations do not follow simple Brillouin functions but have anomalous temperature dependences. We now consider other evidence that an anomalous temperature dependence does exist.

Accompanying antiferromagnetic ordering in MnO and NiO is a small crystallographic distortion which increases as the temperature decreases.<sup>16</sup> Néel<sup>17</sup> first indicated that the sensitivity of the exchange interaction to interatomic distance provides a mechanism, whereby the free energy of a magnetic crystal can be lowered because of a spontaneous crystal distortion. The lattice distortion decreases the free energy by lowering the exchange energy by more than it increases the strain energy. Bean and Rodbell<sup>18</sup> have indicated

how this lattice contraction can, in some cases, strongly influence the temperature dependence of the sublattice magnetization. They find that the spontaneous magnetization in the strained case is always larger at a given temperature than in the unstrained case. A simple point of view is that the increased exchange constant in the strained material gives rise to an apparently higher ordering temperature at absolute zero which decreases, approaching the actual ordering temperature  $T_N$ , as the temperature is raised. The apparent ordering  $T_{N'}$  is related to  $T_N$  by

$$T_{N'} = T_N(1 + \beta\xi),$$

where  $\beta = T_N^{-1}(\partial T_N / \partial \xi)$  and  $\xi$  is a strain parameter.

The x-ray diffraction work of Rooksby<sup>19</sup> and the measurement of the thermal expansion coefficients by Foëx<sup>20</sup> have determined the magnitude of the lattice deformation due to the exchange magnetoelastic coupling in MnO and NiO. If we take the fractional change in volume as the strain parameter, then  $\beta$  can be determined, since the strain is proportional to  $\beta$  times the square of the sublattice magnetization.<sup>18</sup> For MnO the fractional lattice contraction due to magnetic ordering is  $(\Delta V/V) = 3 \times 10^{-3}$  at 0°K and  $\beta$  turns out to be 3.7. At absolute zero  $\beta\xi \approx 1\%$ ,  $T_{N'} \approx T_N$ , and the distortion produces a negligible effect on  $B_{5/2}(T/T_N)$ . Although the distortion is not the cause of the anomalous temperature dependence, it does monitor the true  $M(T)/M(0)$ . The temperature dependence of the sublattice magnetization as determined by taking the square root of the strain is given in Fig. 4.

An independent measure of the temperature dependence of the sublattice magnetization has been obtained from the intensity of magnetic scattering of neutrons as a function of temperature. The intensity of the neutron diffraction from the (111) planes in MnO has been measured by Shull *et al.*<sup>21</sup>  $M(T)/M(0)$  is given by the square root of the neutron intensity. The temperature dependence of the sublattice magnetization as given by neutron intensity is compared with that deduced from crystal strain and also with  $B_{5/2}(T/T_N)$  in Fig. 4.

For the case of NiO, we again have two estimates of the temperature dependence of the sublattice magnetization, both neutron-intensity and thermal expansion data. Roth has measured the intensity of the scattering from (111) planes in nickel oxide as a function of temperature, and he finds that the neutron intensity does not vary as the square of  $B_1(T/T_N)$  but has a somewhat slower rolloff.<sup>22</sup> We have taken the square root of Roth's neutron-intensity data for the sublattice magnetization and compared it to the thermal contraction in nickel oxide as obtained by Slack<sup>23</sup> from the

<sup>12</sup> M. Tinkham, *J. Appl. Phys.* **33**, 1248 (1962).

<sup>13</sup> C. Zener, *Phys. Rev.* **96**, 1335 (1954).

<sup>14</sup> J. H. Van Vleck, *J. Phys. Radium* **20**, 124 (1954).

<sup>15</sup> T. Nagamiya, K. Yosida, and R. Kubo, in *Advances in Physics*, edited by N. F. Mott (Taylor and Francis, Ltd., London, 1955), Vol. 4, p. 14.

<sup>16</sup> N. C. Tombs and H. P. Rooksby, *Nature* **165**, 442 (1950).

<sup>17</sup> L. Néel, *Ann. Phys. (Paris)* **8**, 237 (1937).

<sup>18</sup> C. P. Bean and D. S. Rodbell, *Phys. Rev.* **126**, 104 (1962).

<sup>19</sup> H. P. Rooksby, *Acta Cryst.* **1**, 226 (1948).

<sup>20</sup> M. Foëx, *Compt. Rend.* **227**, 193 (1948).

<sup>21</sup> C. G. Shull, W. A. Strauser, and E. O. Wollan, *Phys. Rev.* **83**, 333 (1951).

<sup>22</sup> W. L. Roth, *Phys. Rev.* **111**, 772 (1958).

<sup>23</sup> G. A. Slack, *J. Appl. Phys.* **31**, 1571 (1960).

thermal expansion data of Foëx. These two sets of data are compared with  $B_1(T/T_N)$  in Fig. 5. Slack finds  $\Delta V/V = 4.5 \times 10^{-3}$  at  $0^\circ\text{K}$ ; hence  $\beta = 1.5$  for NiO. Since  $\beta\xi \approx 1\%$ , we again find  $T_N' \approx T_N$ .

An inspection of Figs. 4 and 5 strongly supports our contention that  $M(T)/M(0)$  is very different from  $B_S(T/T_N)$  in these antiferromagnets. The reason for this large difference is presently not known.

We take the neutron data as the most accurate determination of  $M(T)/M(0)$  and now compare antiferromagnetic resonance theory with our experimental results. The Zener approximation<sup>24</sup> for the temperature dependence of the anisotropy constant for complete correlation of spins,  $n = \frac{3}{2}$ , fits the MnO data up to  $\sim 0.75 T_N$ , with  $M(T)/M(0)$  as determined by neutron diffraction data (see Fig. 2). Above this temperature, the experimental curve approaches the dependence predicted by the molecular-field approximation,  $n = 1$ .

The Zener approximation now also fits the NiO data up to  $\sim 0.75 T_N$  for  $M(T)/M(0)$  determined by neutron diffraction data (see Fig. 3). Again at higher temperatures, the experimental points tend toward the dependence predicted by the molecular-field theory.

Physically, the change in power law of the temperature dependence of the anisotropy constant at high temperatures describes the fading of correlation between neighboring spins, as the temperature is raised. The molecular-field approximation represents the no correlation extreme. It is interesting to note that the Zener approximation (with the slight modifications discussed by Carr<sup>24</sup>) describes the correct temperature dependence over most of the ordered range.

The experimental results strongly suggest that  $B_S(T/T_N)$  does not always describe  $M(T)/M(0)$  in a solid. A case in point is perhaps  $\text{MnF}_2$  vs  $\text{MnO}$ . The function  $B_{5/2}(T/T_N)$  describes reasonably well the temperature dependence of the sublattice magnetization in the former antiferromagnetic material<sup>25</sup> but not in the latter. Aside from the anomalous temperature dependence of the magnetization, there appears to be quantitative agreement of theory, as given by the two

<sup>24</sup> We have used a slight modification of the Zener approximation which has been described in detail by W. Carr, Phys. Rev. **109**, 1971 (1958).

<sup>25</sup> R. Erickson, Phys. Rev. **90**, 779 (1953).

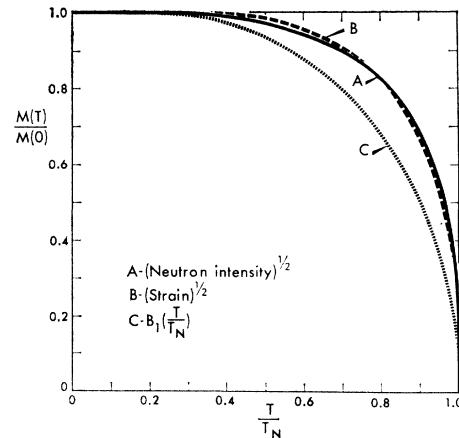


FIG. 5. Temperature dependence of the sublattice magnetization in NiO as given by the square root of the neutron-intensity data and the square root of the magnetoelastic strain.  $B_1(T/T_N)$  is shown for comparison.

sublattice model, and experiment. Thus, although we have not observed the low-frequency mode, some qualitative statements with respect to its properties may be in order.

Because of the polarized nature of the antiferromagnetic modes, each contributes to the perpendicular static susceptibility in orthogonal directions. The low-frequency mode contributes to the perpendicular static susceptibility along the hard axis, whereas the high-frequency mode contributes to the susceptibility along an easy axis. Also the strength of the low-frequency mode is proportional to the square root of the in-plane anisotropy constant or proportional to the resonance frequency itself. Finally, because the in-plane anisotropy for the low-frequency mode is given by a polynomial of order 6, the temperature dependence of the resonance frequency should vary roughly as the tenth power of the sublattice magnetization.

#### ACKNOWLEDGMENTS

The authors have benefited greatly from discussions with Professor F. Keffer. Thanks are also due to Professor K. Yosida for supplying the NiO single crystal grown by Y. Nakazumi (of the Tohichi Chemical Industrial Company, Ltd., Osaka, Japan).